Interferometric Control of Spin-Polarized Electron Populations at a Metal Surface Observed by Multiphoton Photoemission

Aimo Winkelmann,[1,*] Wen-Chin Lin,[1] Francesco Bisio,[2] Hrvoje Petek,[3,4] and Jürgen Kirschner[1]

[1]*Max-Planck Institut für Mikrostrukturphysik, Weinberg 2, D-06120 Halle (Saale), Germany*

[2]*CNISM, Sede consorziata di Genova, Dipartimento di Fisica, via Dodecaneso 33, I-16146 Genova, Italy*

[3]*Department of Physics and Astronomy, University of Pittsburgh, Pittsburgh, Pennsylvania 15260, USA*

[4]*Donostia International Physics Center DIPC, P. Manuel de Lardizabal 4, 20080 San Sebastian, Spain*

(Received 17 January 2008; published 22 May 2008)

In an interferometric pump-probe experiment, we demonstrate the phase tuning of the spin polarization of photoelectrons emitted in a three-photon process from Cu(001). A phase shift of π between delayed ultrafast circularly polarized light pulses can switch the spin polarization from $\pm 20\%$ to $\mp 40\%$. In the delay regime of overlapping pulses, we show the dominating role of optical interference effects in determining the spin polarization. For longer delays, we detect the influence of the coherent material response, manifested in both the final state electron population as well as the final state spin polarization.

DOI: 10.1103/PhysRevLett.100.206601 PACS numbers: 72.25.Fe, 73.20.−r, 78.47.J−, 79.60.−i

The interaction of circularly polarized light with electronic states that are influenced by spin-orbit coupling provides a mechanism for selective excitation of spin-polarized electrons in nonmagnetic and magnetic solids. This type of interaction bears close analogy to the effect of a magnetic field, and it enables the control of magnetic and other spin-dependent phenomena by optical means on time scales of the order of the applied laser pulse lengths and electron-hole pair dephasing times in solids and at solid surfaces. For example, a method of all-optical magnetic recording using circularly polarized 40 fs laser pulses has recently been demonstrated [1]. The successful application of the spin degree of freedom in future spintronic devices [2] equally relies on a fundamental understanding of how to create and manipulate spin-polarized electrons—potentially on ultrafast time scales.

From a fundamental point of view, a particularly direct way to study the relevant mechanisms is to optically excite unoccupied electronic states and then detect spin-polarized photoelectrons emitted from crystalline surfaces. Using nonlinear photoemission in a pump-probe configuration, one can gain access to the electron and spin dynamics in excited states [3–8]. It clearly would be of fundamental interest to elucidate mechanisms by which not only the number but also the spin of the emitted photoelectrons could be influenced by the relative optical phase of two excitation pulses. Ultimately, this could also allow the generalization of the recently demonstrated all-optical control of charge currents on surfaces [9] to spin-polarized surface currents. The steering of the electron's spin, charge and spatial degrees of freedom at surfaces could then be observed directly by spectroscopic and imaging techniques based on photoemission [10–12] to allow fundamental insights, which are relevant in the ineluctable convergence of the optical, electronic and spintronic technologies on the nanometer scale.

In this Letter, we show that the spin-polarized photoemission from the Cu(001) surface can be controlled by interferometrically changing the delay between two circularly polarized ultrashort optical pulses. We exploit a two-photon resonant transition [13] to selectively populate the $n = 1$ image potential (IP) state with spin-polarized electrons originating from the spin-orbit split Cu d-bands [14] and then detect the IP state population and spin polarization by a third photon. Comparing the time-resolved three-photon photoemission (3PPE) signal with a simultaneous measurement of the surface second-harmonic generation (SSHG) signal, we show that the spin-polarized photoemission is influenced by the effective optical excitation spectrum and by the quantum-mechanical response of the excited system.

The experimental setup is schematically pictured in Fig. 1. We have described most of the experimental details previously [13,14]. In the present study, the ultrashort excitation pulses ($h\nu = 3.00 \ldots 3.14$ eV, pulse length <20 fs, pulse energy ~ 1 nJ) were split into equal pump and probe replicas in a stabilized scanning Mach-Zehnder interferometer. The delay could be kept stable with an accuracy of $\lambda/25$. The electrons photoemitted along the surface normal were analyzed angle-resolved by a cylindrical sector analyzer coupled with a spin detector based on very low energy electron scattering on a magnetized ultrathin Fe/W(001) film. The analyzer energy resolution was set to 100 meV. To determine the laser pulse autocorrelation, simultaneously with 3PPE, we measured the surface SHG signal from the Cu(001) sample using a prism assembly to separate the SHG signal from the fundamental light before detection with a photomultiplier tube (Fig. 1). A clean and ordered Cu(001) surface was prepared by standard procedures. The optical plane was aligned parallel to the [100] direction.

In Fig. 2(a) we show the relativistic bulk band structure of the Cu(001) surface along the surface normal (ΓX) direction, whereas a simplified level scheme accounting for the mechanism of spin-polarized 3PPE [14] is reported in Fig. 2(b). According to optical selection rules, oppo-

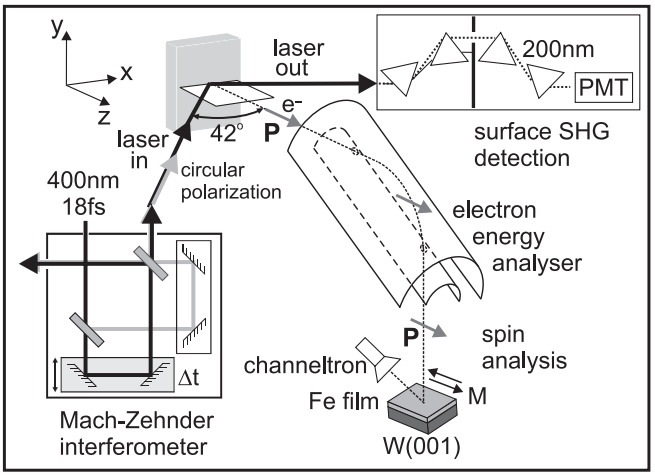

FIG. 1. Experimental setup for interferometric control of spin-polarized electron populations in multiphoton photoemission.

sitely spin-polarized electrons can be excited by circularly polarized light from the d bands of Cu with Δ_7 and Δ_6 symmetry. The two-photon resonance between these initial states, the intermediate unoccupied sp-band, and the penultimate $n = 1$ image potential state in the 3PPE process governs the distribution of spin-polarized electrons at the final state energy. As can be seen in Fig. 2(b), two different resonances take place at photon energies $h\nu_1$ and $h\nu_2$. This leads to the features A and B in the photoelectron spectrum shown in Fig. 2(c). The separation of 150 meV between A and B is determined by spin-orbit coupling, which causes the splitting of the Δ_7 and Δ_6 bands. Because the pulses have a spectral width of 170 meV, both resonances of opposite spin polarization are excited simultaneously weighted by the spectral distribution of excitation frequencies. In principle, the spin polarization detected via the IP state as a function of pump-probe delay can change due to a combination of spin-dependent excitation effects and spin-dependent scattering in the excited state. With measured values of the spin-flip lifetime in bulk copper of about 10 ps [15] we can expect that spin-flip processes in the excited state are not significant in our measurements.

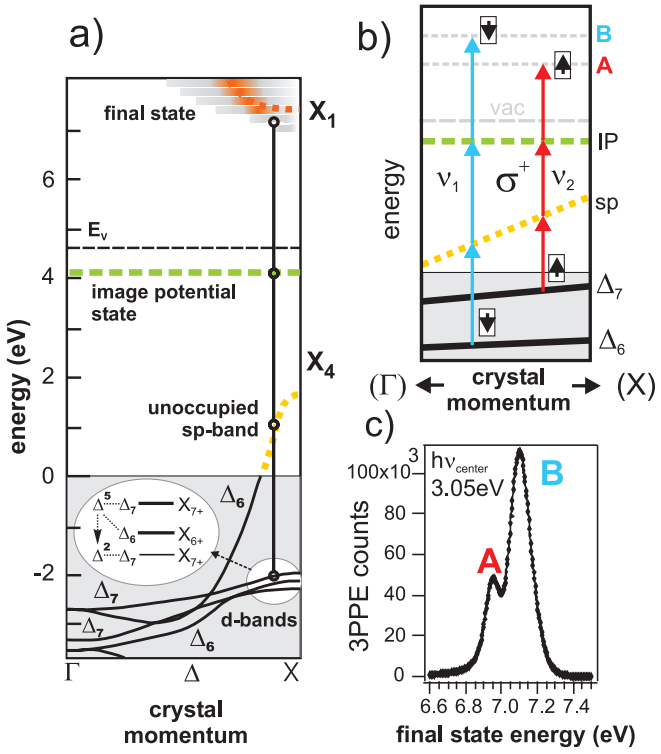

FIG. 2 (color). (a) Relativistic band structure relevant to normal emission from Cu(001), (b) Qualitative excitation scheme for spin-polarized 3PPE using pulses with a frequency spectrum covering ν_1 and ν_2 (σ^+ right circular polarized light), (c) 3PPE resonance peak measured in a non-spin-resolved experiment with higher energy resolution directly showing the spin-orbit splitting of the two resonances A and B.

The time-resolved experiments can be carried out in two ways. Measuring the photoelectrons at a fixed energy as a function of delay between the pulses gives an interferometric two-pulse correlation (I2PC) signal, while measuring the photoelectron intensity at fixed pulse delays as a function of photoelectron kinetic energy gives the corresponding energy and spin polarization control spectra. We will begin by discussing the observed spin polarization for pulse delays up to about 15 fs (Fig. 3). At these delays, the pulses are overlapping significantly so that the optical interference of the electromagnetic fields of the two constituting pulses dominantly determines the measured signal [16]. As a function of pulse delay, this results in interference maxima spaced in time by the duration of an optical cycle.

In the top part of Fig. 3, we report the spin polarization measured at the final state energy of 6.95 eV above the Fermi energy E_F with $h\nu = 3.04$ eV, as a function of the pulse delay. Each data point for the spin polarization is shown in a gray scale corresponding to its statistical error, where black points correspond to the minimum error. Data points on the white end of the scale are effectively suppressed, as they fall in the regions of destructive interference where the count rate is too low for a statistically significant result. The spin polarization exhibits dramatic oscillations with a frequency of about 1.3 fs^{-1} which corresponds to an optical cycle. Starting from about +10% at zero delay, the amplitude of the polarization oscillations also grow larger in intensity, reaching values ranging from +40% to −20% for delays between 10 and 15 fs.

Additional insights into this oscillating behavior can be gained by measuring spin-resolved photoelectron spectra at selected fixed delays within one representative optical cycle. In the bottom part of Fig. 3, we therefore report the intensity spectra (hatched areas) and the corresponding spin polarizations (markers) obtained for delays near 11 optical cycles, along with the reference zero-delay results. Whereas the spin polarization spectrum at zero delay perfectly agrees with our previous study [14], marked changes are observed in the spin polarization spectra for the chosen

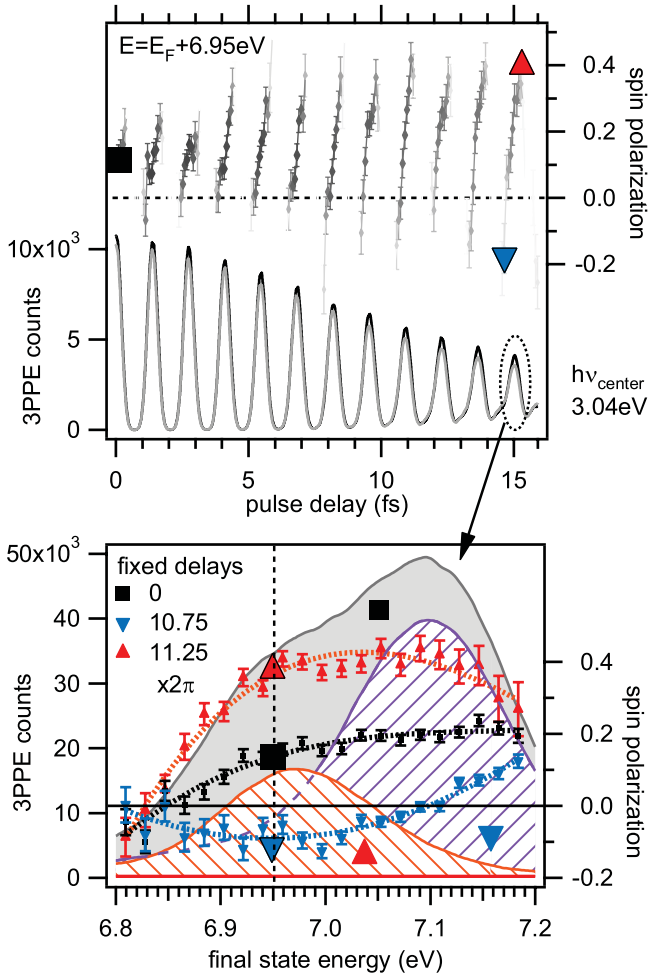

FIG. 3 (color). Top panel: spin polarization (markers with error bars) and corresponding interferometric 3PPE signals for reversed magnetizations of the spin detector (solid lines) at the final state energy $E = 6.95$ eV as a function of pulse delay. Data points for the spin polarization with lower error are colored darker (see text). Bottom panel: measured spin polarization as a function of final state energy for selected fixed pulse delays of 0, 10.75, and 11.25 optical cycles (markers with error bars). The lines are guides to the eye. The gray shaded and hatched areas in the background show the spin-averaged three-photon photoemission spectra at delays of 0, 10.75 and 11.25 optical cycles, respectively.

values of pulse delay. In agreement with the upper part of the figure, at 6.95 eV final state energy we observe a spin polarization near -20% for 10.75 cycles and $+40\%$ near 11.25 optical cycles delay. The connection to the upper part of the figure is made by the colored symbols in both parts of Fig. 3.

The dramatic changes in the spin polarization spectra become clear when we compare the spin-averaged intensity spectra for different delays. It can be seen in fact that at zero delay, the spin-averaged intensity spectrum (gray spectrum in bottom part of Fig. 3) is relatively broad, caused by the nearly equal excitation of the A and B resonances by our ultrashort pulses with an extended frequency spectrum. When the two pulses are delayed by less than their pulse width and thus still significantly overlapping, their superposition can be effectively viewed as a single, longer pulse, whose amplitude and frequency structure is determined by the interference of the overlapped pulses. For delays of only one or two optical cycles, the pulses are still almost completely overlapping. This leads to almost total destructive and constructive interference of all frequency components, causing the high interference contrast near zero delay in the I2PC curves in the upper part of Fig. 3. The spin polarization is only mildly influenced at these very short delays with respect to the zero-delay case because the *complete* frequency spectrum of the pulse pair is alternately enhanced or suppressed, without preferential excitation of the A or B resonance. This gradually changes at longer pulse delays (> 3 optical cycles), when the decreasing overlap between the pulses causes a more complicated frequency interference that, advancing the delay by an optical cycle, leads to spectral distributions that are markedly asymmetric with respect to the original pulse spectra. Thus, under these conditions, changing the delay by less than an optical cycle, we can correspondingly change the spectrum of two combined pulses to preferentially excite resonance A or resonance B. As is apparent from the red and the blue hatched intensity spectra in the bottom part of Fig. 3, the constructive and destructive interferences between the different spectral components of the excitation light at, respectively, 10.75 and 11.25 cycles delay occur at opposite sides of the original spectrum. In effect, the spectral maximum corresponding to the constructive interference between the two pulses is shifted towards higher or lower energies depending on the selection of the relative phase. The excitation energy is known to strongly affect the spin polarization measured from the $n = 1$ IP state [14]. What we therefore accomplish in our time-resolved experiment is the control of this spin polarization via a preferential selection of one or the other of the two simultaneous resonances A or B, obtained by a change of the effective optical spectrum in the course of the coherent nonlinear excitation.

We have demonstrated that, for strongly overlapping pulses, an effective optical spectrum can be viewed as dominant in determining the observed 3PPE spin polarization oscillations. When the two pulses are delayed by intervals longer than their pulse width, however, the time development of the excited quantum-mechanical system has to be taken into account appropriately. The evolution and possible decay of the polarization phase between the action of the two pulses determines how the phase information imprinted by the pump pulse is transmitted over time to result in the interference with the probe pulse. Qualitatively, the nonlinear material response results in the appearance of additional frequencies in the interferometric correlation signal [17]. In order to probe this regime, in Fig. 4, we report time-dependent measurements of the 3PPE spin polarization recorded with a central photon energy of 3.09 eV for pulse delays between 42 and 46 fs,

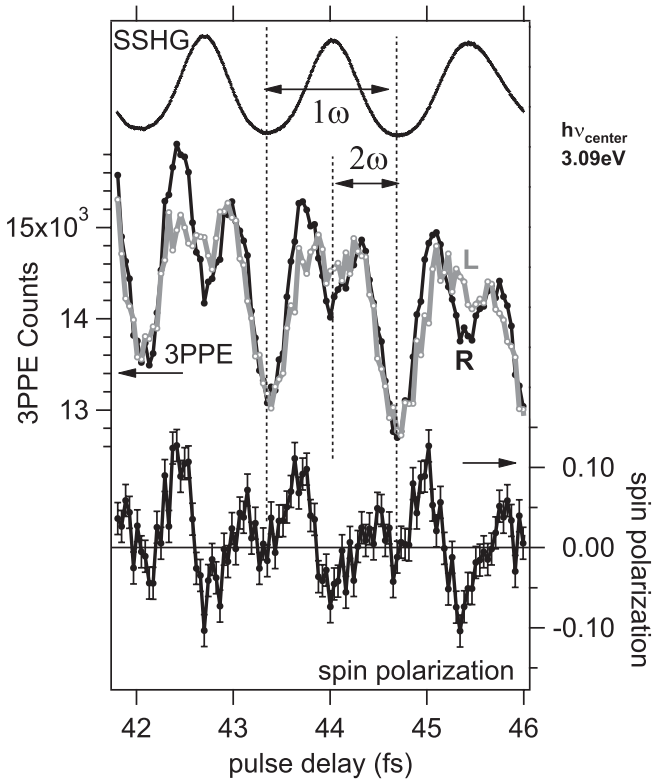

FIG. 4. Top: SSHG intensity measured as a function of the pulse delay. Middle: 3PPE signal as a function of the pulse delay (L/R are data measured for reversed magnetization of the spin detector). Bottom: spin polarization extracted from the L/R curves. The presence of oscillations in the 3PPE signal and spin polarization at the frequency 2ω is highlighted. Data were measured with $h\nu = 3.09$ eV photon energy.

times which are sufficiently longer than the pulse width. In the top part of Fig. 4, the autocorrelation signal obtained by SSHG is reported, clearly showing oscillations at the fundamental frequency ω corresponding to one optical cycle of delay. In the center of the figure, we report the 3PPE signal measured at $E = E_F + 6.95$ eV for the two orientations of the magnetization of the Fe film in the spin detector (R/L in Fig. 4), and the relative spin polarization (bottom). Under these excitation and measurements conditions, we notice that the average spin polarization is near zero and can be changed to positive as well as to negative values by the pulse delay. When we compare the 3PPE signal with the simultaneously measured SSHG, we notice that clear oscillations at twice the optical frequency appear, which originate from the coherent nonlinear response characterized by dephasing times the of the d-band holes of about 30 fs [18,19] and the image potential state lifetimes of about 35 fs [5]. The same 2ω contribution is also seen clearly in the spin polarization. By this observation of the appearing 2ω contributions, we directly demonstrate that the phase of the material polarization affects the photoelectron spin polarization in the regime of delayed pulses which are separated by delays sufficiently larger than the temporal pulse width but within the relevant dephasing time scales of the excited system. Because the observed spin polarization is a function of the relative excitation of the A and B resonances which are originating from different d bands, the additional spin information in principle gives the possibility to extract band-resolved dephasing times of d-band holes and to monitor band-resolved population dynamics.

In summary, we reported the interferometric control of the spin polarization of photoelectrons by changing the delay between two ultrashort optical pulses. Our results show that the study of coherent electron dynamics at metal surfaces can be extended to spin-polarized electron populations. Our studies can be readily generalized to cases involving the control of the time-dependent optical polarization of the excitation pulses [20].

Technical assistance from F. Helbig is gratefully acknowledged. H. Petek thanks the Department of Energy Grant No. DE-FG02-03ER15434 and Ikerbasque for financial support. F. B. acknowledges the CNR-CNISM agreement for financial support.

*winkelm@mpi-halle.mpg.de

[1] C. D. Stanciu *et al.*, Phys. Rev. Lett. **99**, 047601 (2007).
[2] I. Zutić, J. Fabian, and S. D. Sarma, Rev. Mod. Phys. **76**, 323 (2004).
[3] R. Haight, Surf. Sci. Rep. **21**, 275 (1995).
[4] H. Petek and S. Ogawa, Prog. Surf. Sci. **56**, 239 (1997).
[5] M. Weinelt, J. Phys. Condens. Matter **14**, R1099 (2002).
[6] M. Aeschlimann *et al.*, Phys. Rev. Lett. **79**, 5158 (1997).
[7] A. B. Schmidt *et al.*, Phys. Rev. Lett. **95**, 107402 (2005).
[8] M. Weinelt *et al.*, Prog. Surf. Sci. **82**, 388 (2007).
[9] J. Güdde *et al.*, Science **318**, 1287 (2007).
[10] M. Cinchetti *et al.*, Phys. Rev. Lett. **95**, 047601 (2005).
[11] A. Kubo, N. Pontius, and H. Petek, Nano Lett. **7**, 470 (2007).
[12] M. Aeschlimann *et al.*, Nature (London) **446**, 301 (2007).
[13] F. Bisio *et al.*, Phys. Rev. Lett. **96**, 087601 (2006).
[14] A. Winkelmann *et al.*, Phys. Rev. Lett. **98**, 226601 (2007).
[15] F. J. Jedema, A. T. Filip, and B. J. van Wees, Nature (London) **410**, 345 (2001).
[16] V. Blanchet *et al.*, Phys. Rev. Lett. **78**, 2716 (1997).
[17] H. Petek *et al.*, Phys. Rev. Lett. **79**, 4649 (1997).
[18] S. Ogawa *et al.*, Phys. Rev. Lett. **78**, 1339 (1997).
[19] H. Petek, H. Nagano, and S. Ogawa, Phys. Rev. Lett. **83**, 832 (1999).
[20] A. P. Heberle *et al.*, IEEE J. Sel. Top. Quantum Electron. **2**, 769 (1996).